Composites Science and Technology 74 (2013) p. 113-120.
http://dx.doi.org/10.1016/j.compscitech.2012.10.013

Stress concentrations in an impregnated fibre bundle with random fibre packing

Y. Swolfs*, L. Gorbatikh, V. Romanov, S. Orlova, S.V. Lomov, I. Verpoest
Department of Metallurgy and Materials Engineering (MTM), KU Leuven, Kasteelpark Arenberg 44, B-3001 Heverlee, Belgium
*Corresponding author. Tel.: +32 16 32 12 31; fax: +32 16 32 19 90
E-mail address: yentl.swolfs@mtm.kuleuven.be (Y. Swolfs)

Abstract
The stress redistribution after a single fibre break is a fundamental issue in longitudinal strength models for unidirectional composites. Current models assume hexagonal or square fibre packings. In the present work, random fibre packings were modelled using 3D finite element analysis and compared to ordered fibre packings. Significant differences in the stress redistribution are found. Compared to square and hexagonal packings, random fibre packings result in smaller stress concentration factors for fibres at the same distance from the broken fibre. These random packings, however, also show higher maximal stress concentration factors. The influence of the fibre breakage is more localised, which results in lower ineffective and overload lengths. The presence of fibres at smaller distances from the broken fibre explains these phenomena. For an accurate representation of the stress redistribution after a fibre breakage, random fibre packings should be used.

Keywords
A. Polymer-matrix composites (PMCs), C. Stress concentrations, C. finite element analysis, ineffective length

1 Introduction

A fundamental understanding of the failure of fibre-reinforced composites is crucial for their widespread application as it improves their overall performance and helps in designing better parts. The failure process of unidirectional fibre-reinforced composites is now reasonably well understood [1-3]. When a fibre breaks, it locally loses its load transfer capability. The surrounding matrix is loaded in shear and transfers the load back onto the broken fibre. Hence, the fibre recovers its stress and the length over which this occurs is called the ineffective length. Near the broken fibre, the stress in the surrounding fibres is increased. This increase in stress is quantified using the stress concentration factor (SCF), which is the relative increase in stress in the neighbouring fibres due to the fibre breakage of one fibre. SCFs increase the probability of fracture of the neighbouring fibres. When enough neighbouring fibres are broken, a critical cluster size is reached and catastrophic failure occurs. This failure propagation scheme shows the importance of the stress distribution after a fibre fracture. The ineffective length and the SCF are crucial parameters to predict the strength of unidirectional composites.

Shear lag models (SLM) were developed to calculate this stress redistribution. They assume that the fibres carry all the axial loads and the matrix only the shear loads. The first SLM was developed by Hedgepeth for a 1D packing [4]. A 1D packing is a single-

layer arrangement of parallel fibres on a straight line. Hedgepeth predicted a SCF of 33% for this case [4]. Later, Hedgepeth and Van Dyke [5] extended the SLM to 2D packings, which consist of a planar arrangement of parallel fibres. The authors calculated a SCF of 14.6% and 10.4% for square and hexagonal 2D packings, respectively. SLMs are straightforward to incorporate into an analytical strength model, as they give an analytical solution for the stress redistribution after a fibre breakage. Combining SLM with a Weibull strength distribution and some assumptions can give an analytical solution for the strength of unidirectional composites [6, 7]. However, SLM also has several disadvantages: (1) it does not include matrix plasticity, (2) it does not allow anisotropic properties of fibres, (3) it cannot predict matrix cracking, (4) it assumes perfect fibre-matrix bonding, and (5) it assumes an ordered packing. Many authors have published improvements on these issues [8-13]. The SCF has in all cases been estimated to be lower than Hedgepeth's prediction [4, 5].

An alternative approach to calculate the stress redistribution after a fibre breakage is to use 3D finite element models (FEM). 3D FEM is computationally intensive, which limits the amount of fibres that can be included in the model. Therefore, this method on its own is insufficient to predict the full statistical nature of composite failure. The 3D FEM stress redistribution after a fibre breakage can however be used as input for strength models [3]. Nedele and Wisnom [14] predicted a SCF of 5.8% for a hexagonal packing of carbon fibres. This represents a much lower value than the 10.4% predicted by Hedgepeth and Van Dyke [5]. Moreover, Xia et al. [15] showed that the fibre shear deformation, which is neglected in SLMs, can affect the stress redistribution after a fibre breakage. Furthermore, van den Heuvel et al. [16] experimentally validated the accuracy of the 3D FEM approach for calculating SCFs in a microcomposite with five fibres. Good agreement was found between micro-Raman spectroscopy and 3D FEM calculations. Small discrepancies were found only at small fibre spacings.

Batdorf and Ghaffarian [17] noticed a significant discrepancy between experimental and modelling results of strength of unidirectional composites. The authors indicated that the major cause for this discrepancy was the variation in fibre spacing. Incorporation of the statistical variation of fibre spacing led to a smaller discrepancy between experiment and model. The authors themselves realised the limitations of their model and suggested more work was needed to confirm this hypothesis. The number of shear lag models for a random fibre packing is limited. Only a few studies have addressed this issue [8, 18, 19]. Even though all these models were limited to 1D packings, it showed that SCFs should be approached in a statistical manner. To the authors' best knowledge, no SCFs values have been reported for 2D random fibre packings, neither for SLM nor for 3D FEM. This can be explained by the inherent difficulty in creating 2D random fibre packings, which are statistically equivalent to fibre packings in real fibre-reinforced composites. Several models are limited to fibre volume fractions of less than 55% [20], which is too low for unidirectional fibre bundles. Some models are capable of reaching higher fibre volume fraction, however, these were not analysed statistically [21, 22].

The present paper shows 3D FEM results for stress concentration factors in random 2D fibre packings. An adapted version of the algorithm of Melro et al. [23] was used to generate random fibre packings. This algorithm is capable of reaching fibre volume fractions of more than 70%, with a high degree of randomness [24]. After proving the

computational validity of the model, it will be illustrated that SCFs depend on the type of fibre packing. The influence of fibre volume fraction and fibre/matrix stiffness ratio will also be investigated. Finally, the importance of using anisotropic elastic properties of fibres will be shown.

2 Description of the model

2.1 Procedure

Firstly, a random fibre packing model is generated. The basic principles of the used generator are described in [23]. The algorithm requires three input parameters: the fibre radius, the fibre volume fraction and the size of the representative volume element (RVE). The first step is a hard-core algorithm, which adds fibres at random coordinates within a square RVE as long as the fibres do not touch each other. This step is limited to a fibre volume fraction of about 55%. The second step tries to move each fibre closer to its nearest, second nearest and third nearest neighbour. The third and final step pushes the fibres on the edges of the RVE inwards. These three steps are repeated until the required fibre volume fraction is achieved. A criterion for the minimal fibre distance was added. In the original algorithm [23], the minimal distance between the fibre centres is two times the fibre radius. This criterion was adapted to randomly generate the minimal distance in the interval between 2 and 2.1 times the fibre radius. This adaptation increases the similarity of the statistical descriptors between generated and real fibre distributions [24].

Secondly, the finite element model is created using the generated random fibre packing. A circular model is cut out of the square RVE (see figure 1a). In contrast with the square or hexagonal packings [14, 25, 26], a random packing model cannot be reduced to one-eighth or one-twelfth of the model (like in square or hexagonal models) due to lack of symmetry. Even for the reference square and hexagonal models, the full 360° model was deliberately chosen to avoid any impact on the results. The applied boundary conditions are shown in figure 1b. The entire top plane is displaced vertically with a strain of 0.1%, while z-symmetry is applied to the bottom plane. This z-symmetry is not applied to the middle fibre, which represents a fibre breakage. Traction free boundary conditions are applied to the lateral surface of the cylinder. This set of boundary conditions has been used previously to represent a unidirectional composite with one broken fibre [25]. Linear elasticity and perfect bonding are assumed for matrix and fibres. More details about the model can be found in Table 1.

Composites Science and Technology 74 (2013) p. 113-120.
http://dx.doi.org/10.1016/j.compscitech.2012.10.013

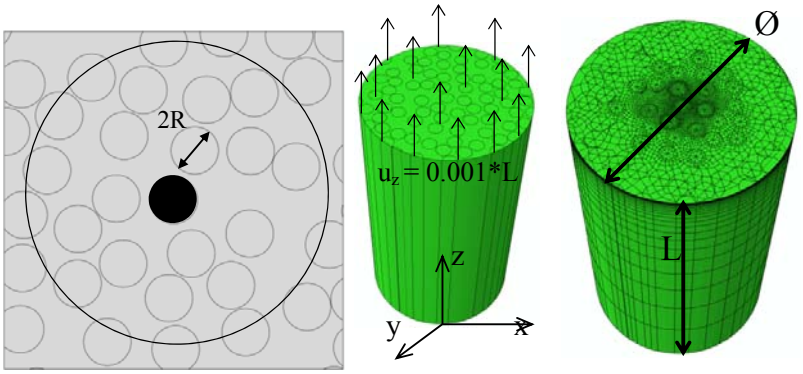

(a) (b) (c)

Figure 1: Description of the model: (a) Creation of a circular model out of the square RVE, with the broken fibre indicated in black (b) boundary conditions (c) 3D view of the mesh

Table 1: Parameters of the finite element model

Fibre radius	3.5 µm
Length L of RVE (see Figure 1c)	40*R
Diameter Ø of RVE (see Figure 1c)	24*R
Number of fibres	42-51 fibres for V_f = 30% 79-84 fibres for V_f = 50% 116-122 fibres for Vf = 70%
Number of elements	> 180000 elements
Type of elements	70-90% second-order brick elements 10-30% second-order wedge elements

Finally, the necessary data are extracted out of the stress field. The stress field in a cross-section through a fibre is not constant (see figure 2). The average fibre stresses will be used rather than the peak stresses. This is more relevant for application in strength models in the future.

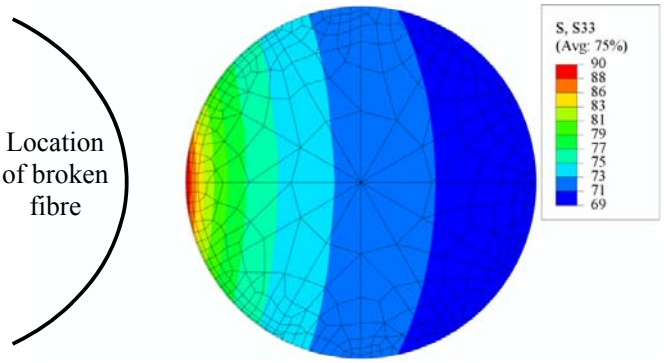

Figure 2: The longitudinal stress field of an intact glass fibre near a broken glass fibre in the crack plane. The applied strain is 0.1% and fibre volume fraction 70%.

Composites Science and Technology 74 (2013) p. 113-120.
http://dx.doi.org/10.1016/j.compscitech.2012.10.013

Within each fibre, the average stress is calculated in 25 planes parallel to and at distances $z*$ from the crack plane. In each of these planes, the longitudinal fibre stress is probed in at least 2400 locations and averaged out over the plane, resulting in the average fibre stress $\sigma_{z,avg}$ at $z*$. From this, three parameters are calculated: the ineffective length, the SCF, and the overload length. Firstly, in accordance with Rosen's definition [27], the ineffective length is defined as twice the fibre length over which 90% of strain recovery occurs (see figure 3a). Secondly, the stress concentration factor (SCF) at a certain z-coordinate $z*$ is defined as the relative increase in fibre stress at that point due to the fibre breakage. An equivalent definition by Fukuda [18] was used: the SCF is calculated as the relative increase in average fibre stress $\sigma_{z,avg}$ at $z*$ divided by the average fibre stress $\sigma_{z,avg}$ far away from the failure location.

$$SCF(z=z^*) = \frac{\sigma_{z,avg}(z=z^*) - \sigma_{z,avg}(z=L)}{\sigma_{z,avg}(z=L)}.100\% \qquad \text{(eq. 1)}$$

This assumes that the fibre stress at $z = L$ is not influenced by the broken fibre. This was verified for all models. This definition eliminates the need to calculate the stress field without the fibre breakage, which saves calculation time. An example of the SCF as a function of the distance along the fibre is shown in figure 3b. The SCFs used in the graphs later in this paper are always the peak values along the fibre length.

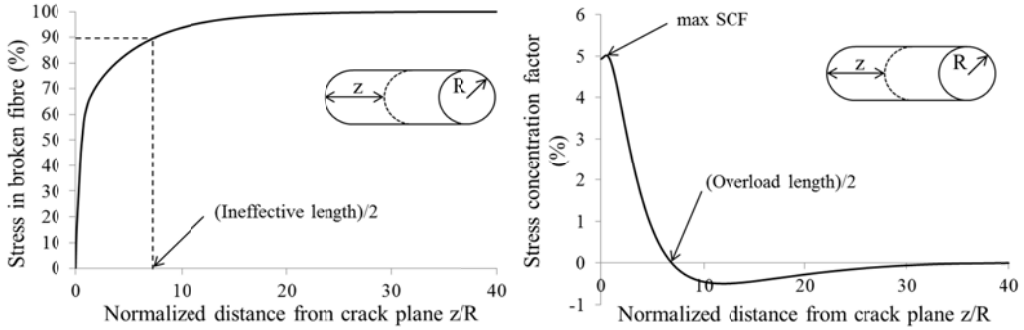

(a) (b)

Figure 3: Definition of (a) ineffective length and (b) overload length and max SCF

Thirdly, the overload length for the intact fibres is calculated similarly to the ineffective length for the broken fibre. This parameter is defined as twice the distance between the crack plane and the plane at which the fibre has a SCF of 0% (see figure 3b). It is a measure for the length over which the stress is increased. This is important, because together with the SCF, it will determine the increase in failure probability of the intact fibres.

2.2 Mesh verification

Highly refined meshes are needed near the stress concentration sites, but these meshes are computationally expensive. To keep the models tractable, the mesh needs to be optimised. Two of these mesh optimisations will be shown here.

The location that requires the highest mesh density is the edge of the broken fibre in the crack plane. If the mesh density is too low, the stress field in the intact fibres will be influenced. The default mesh is shown in figure 4a. To verify whether this mesh is refined enough, the mesh was refined near the fibre surface (see figure 4b). The maximal difference in ineffective length, SCF and overload lengths only amounts to 0.002%. Therefore, the default mesh in figure 4a was used for all models.

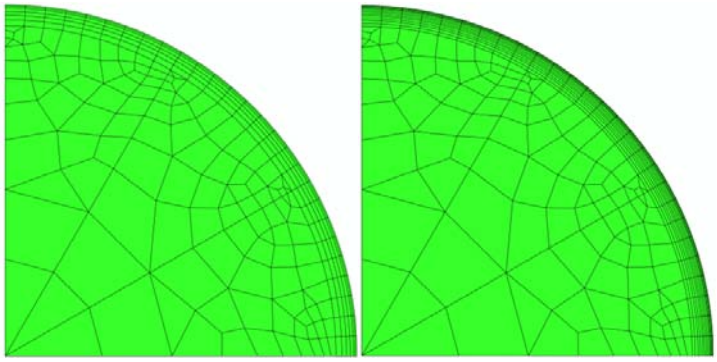

(a) (b)

Figure 4: A quarter of the mesh in the broken fibre (at the crack plane): (a) default mesh (b) refined mesh. Both meshes remain the same along the fibre direction.

The amount of fibres that are included in the models can also influence the results. The diameter Ø of the model (see figure 1c), and the fibre volume fraction determine the amount of fibres included. Since the model diameter is the most critical for a low fibre volume fraction, this mesh optimisation was done for models with 30% fibre volume fraction (referred to as 30% models later in this paper). The diameter Ø was increased from 24*R to 36*R. This changes the ineffective and overload lengths by less than 3%. The relative change in SCF was 1% at most. Therefore, all the model diameters Ø were limited to 24*R. Depending on the fibre volume fraction, this results in a different amount of included fibres (see table 1).

3 Results and discussion

3.1 Fibre packing

This section examines the influence of the fibre packing. Two ordered fibre packings, namely square and hexagonal, are compared to five random fibre packings. The fibre volume fraction is 70% in all cases. This is a realistic fibre volume fraction inside the yarns of textile based composites, but is also present locally in UD-based composites. The model composite consists of glass fibres (stiffness of 70 GPa and Poisson's ratio of 0.22) in an epoxy matrix (stiffness of 3 GPa and Poisson's ratio of 0.4).

Figure 5a shows the ineffective length for the different packings: single values for the square and hexagonal packings, and an average value with standard deviation for the random packing. The random packing has the lowest ineffective length, while the hexagonal packing has the highest ineffective length. These differences are due to differences in the shear stiffness around the broken fibre. The material immediately

surrounding the broken fibre is loaded in shear and transfers the longitudinal stress back on to the broken fibre. In a material with higher shear stiffness, this stress recovery will occur over a smaller length. The shear stresses leading to the stress recovery are mainly located in the material surrounding the broken fibre. Therefore, the shear stiffness of that part of the material will contribute more to the stress recovery. In hexagonal packings, all nearest neighbours of the broken fibre are at the same distance. In random packings, some fibres are almost touching the broken fibre, while others are located further away. If the fibres are closer to each other, the shear stresses in the matrix will be higher than when they are far from each other. This leads to a faster stress build up in the broken fibre away from the crack plane, and hence to a lower ineffective length for random packings (see figure 5a). The ineffective length of square packings is in between the ineffective lengths for random and hexagonal packings. This is because the nearest neighbours in square packings are closer to the broken fibre than in hexagonal packings, but not as close as in random packings.

Figure 5b shows the SCF in the neighbouring fibres for the three fibre packings. It should again be emphasised that these SCFs are calculated based on the average stresses in one plane at distance z* from the crack plane, and hence they underestimate the local stresses, which are higher at the side of the fibre closer to the broken fibre. A strongly decreasing trend is observed as a function of the distance. The data points for the random fibre packings have SCFs of up to 12%. This is almost twice as much as for the square packing and three times as much as for the hexagonal packing. When comparing data points at the same distance to the broken fibre, the ordered packings show higher SCFs. In the hexagonal model, this is even 45% higher than the SCF found for the same d/R in the random models. This is due to the shielding effect. The six nearest neighbours in hexagonal packings shield the second nearest neighbours from the stress concentration. Therefore, the second nearest neighbours show a much lower SCF. A similar, but much stronger shielding effect is found in random packings. The single nearest neighbour in a random packing is much closer to the broken fibre than the six nearest neighbours in a hexagonal packing. This results in SCFs of up to 14% in random packings, as can be seen in figure 5b. Because of these higher SCFs, a larger part of the total overload is already transferred, which results in a smaller overload on the other fibres. Hence, random packings shield the fibres that are further away more efficiently and show a lower SCF for the same normalised distance.

Finally, the overload lengths are shown in figure 5c. Stress concentrations on the intact fibres occur because the broken fibre is not carrying the full load. Therefore, the ineffective length and the overload length follow a similar trend. This can be seen in figure 5c.

Composites Science and Technology 74 (2013) p. 113-120.
http://dx.doi.org/10.1016/j.compscitech.2012.10.013

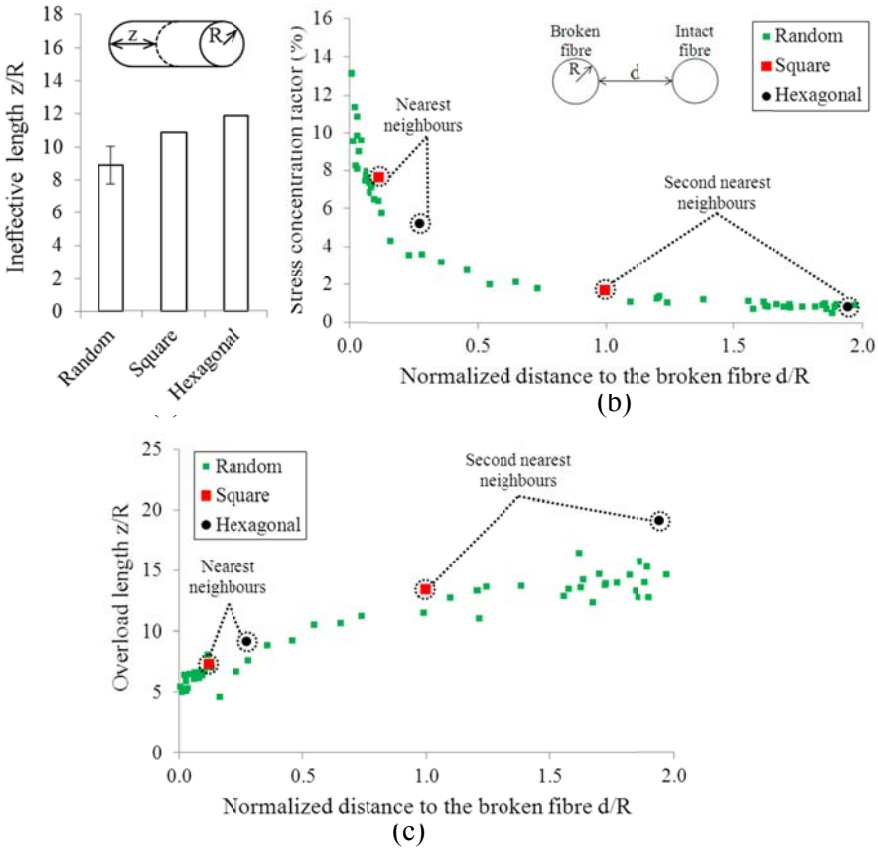

Figure 5: The three parameters describing the stress redistribution in different fibre packings with a fibre volume fraction of 70% (a) ineffective length with error bars for the standard deviation of the 5 random packings, (b) SCF, and (c) overload length.

3.2 Fibre volume fraction

This section examines the influence of fibre volume fraction on the stress concentrations in random fibre packings. The chosen fibre volume fractions are 30%, 50% and 70%. Five packings were examined for fibre volume fractions of 50% and 70%. For 30%, this number was increased to 7 to obtain sufficient data points. The model composite consists of glass fibres (stiffness of 70 GPa and Poisson's ratio of 0.22) in an epoxy matrix (stiffness of 3 GPa and Poisson's ratio of 0.4). The results are shown in figure 6.

Figure 6a shows the results for the ineffective length. The V_f = 70% packings have a much lower SCF than the V_f = 30% and V_f = 50% packings. The V_f = 70% packings have higher shear stresses in the matrix, because they have more fibres at small distances. These higher shear stresses result in a faster stress recovery and thus a lower ineffective length.

Figure 6b shows the results for the SCF. A high fibre volume fraction results in a low SCF for the same distance. The trend line for V_f = 30% is approximately twice as high as for V_f = 70%. This is again due to the shielding effect. A high fibre volume fraction

has more fibres nearby, which results in a stronger shielding effect. Interestingly, previous publications [14-16] concluded that the SCF increases with fibre volume fraction. Figure 6b indicates that the opposite is true for random packings. All previous publications with 2D packings used ordered packings. In these ordered packings, the fibre volume fraction is directly related to the distance between the considered fibre and the broken fibre. In random packings, these two parameters are decoupled. As can be seen in figure 6b, a higher fibre volume fraction results in more fibres at small distances and thus with high SCFs. However, when comparing SCFs at the same distance from the broken fibre (for instance at d/R = 0.5), the higher fibre volume fraction results in a lower SCF.

The overload length again shows the same trend as the ineffective length (see figure 6c). A high fibre volume fraction results in a low overload length.

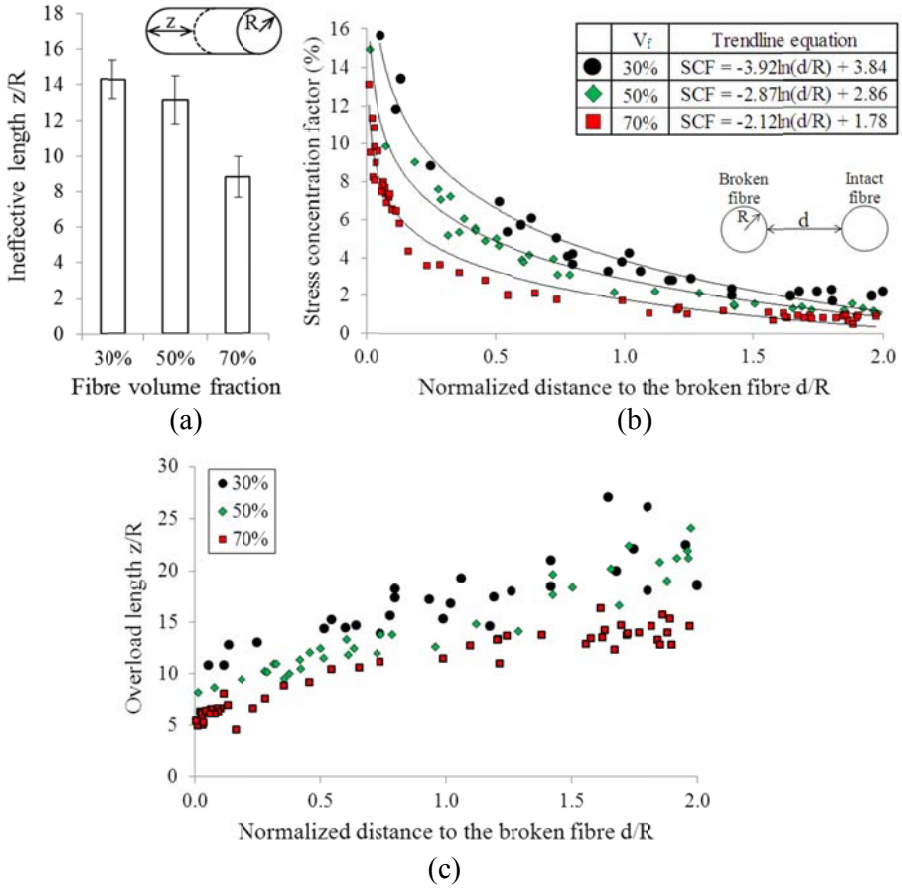

Figure 6: The three parameters describing the stress redistribution for random fibre packings with different fibre volume fractions (a) ineffective length (b) SCF (c) overload length.

3.3 Fibre/matrix stiffness ratio

This section uses three different isotropic fibres. The fibre stiffness is 10, 70 or 230 GPa, while the Poisson's ratio is 0.22 in all cases. The matrix is epoxy, with an isotropic stiffness of 3 GPa and a Poisson's ratio of 0.4. The fibre volume fraction is 70% for all models. Five models were examined for each fibre stiffness.

If the Poisson's ratio is the same, it is expected that a higher fibre stiffness results in higher shear stresses in the matrix in between the fibres. Indeed, shear lag models indicate that a higher stiffness mismatch between fibre and matrix leads to higher shear stresses. Such higher shear stresses should result in a smaller ineffective length. This is clearly not the case in figure 7a. A higher longitudinal fibre stiffness also results in higher stress far away from the crack plane, since the applied strain is the same. Since more stress needs to be transferred onto the broken fibre, the stress recovery will be spread out over a larger distance. The latter effect is more important than the increase in shear stress. The increased fibre shear stiffness only partially affects the shear stresses in the matrix, because those stresses also depend on the matrix shear stiffness and the distance from the broken fibre. Since the matrix occupies most of the volume near the broken fibre, the matrix shear stiffness will dominate the shear stresses. The fibre stiffness only has a small influence on the SCF (see figure 7b). A higher fibre stiffness only slightly increases the shielding effect. For a fibre stiffness of 10 GPa, the matrix can also carry a substantial part of the stress concentration. If the fibre stiffness is a lot higher than the matrix stiffness, the influence of the matrix contribution to the shielding effect diminishes and the SCF increases slightly.

The overload length follows the same trend as the ineffective length (see figure 7c). A higher fibre stiffness results in a higher overload length, because the stress recovery in a stiff fibre requires more stress transfer. This effect is more important than the increased shear stresses in the matrix.

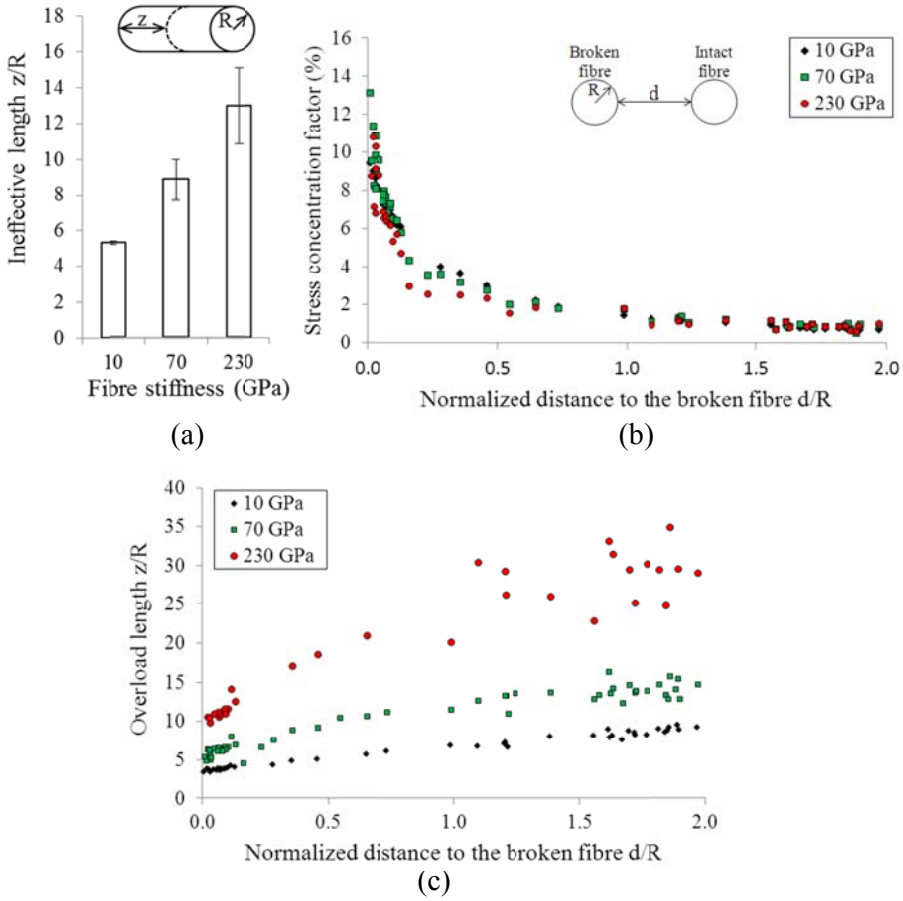

Figure 7: The three parameters describing the stress redistribution for different fibre stiffnesses (a) ineffective length (b) SCF (c) overload length.

3.4 Anisotropy

Most SLMs are not capable of incorporating anisotropic elastic properties. In the case of carbon fibres, this results in a major overestimation of shear modulus of carbon fibre. In previous paragraphs, arguments were developed that the shear stress build up in the matrix is a function of the stiffness mismatch. This predicts a significant influence of the fibre anisotropy on the ineffective length and overload length, but not on the SCF. Three models were analysed for a fibre volume fraction of 30%, 50% and 70%. To avoid cluttering up the graph, the results for only one packing at each fibre volume fraction will be shown. Each of these models was duplicated, with exactly the same mesh, but with two different sets of elastic fibre properties, one isotropic and the other anisotropic. These properties are summarised in table 2. The anisotropic carbon fibre data is based on data in [28, 29]. The matrix is epoxy, with an isotropic stiffness of 3 GPa and a Poisson's ratio of 0.4.

Table 2: Engineering constants of isotropic and transversely isotropic fibres

Fibre type	E_{11} (GPa)	E_{22} (GPa)	E_{33} (GPa)	ν_{12}	ν_{13}	ν_{23}	G_{12} (GPa)	G_{13} (GPa)	G_{23} (GPa)
Isotropic	230	230	230	0.25	0.25	0.25	92	92	92
Transversely isotropic	230	15	15	0.25	0.25	0.25	13.7	13.7	6

The anisotropic carbon fibres have a much lower shear stiffness than the isotropic carbon fibres (see table 2). This results in lower shear stresses in the matrix and thus a higher ineffective and overload length (see figure 8a and c). This increase of the ineffective length is not proportional to the increase in fibre shear stiffness. This is due to the same reason as explained in paragraph 3.3: the matrix is still responsible for a major part of the shear stresses in the matrix region in between two fibres.

Figure 8b shows that anisotropic fibres have a higher SCF for all distances from the broken fibre. The anisotropic fibres have a much lower shear stiffness than the isotropic fibres (see table 2). This lower shear stiffness results in more shear deformation and more stress transfer onto the intact fibres. SLMs assume a zero fibre radius and thus an infinite shear stiffness. This simplification is only justified if the ratio of the fibre and matrix shear stiffness is large. This confirms the findings of Xia et al. [15], where similar effects are noticed. Comparing the SCF values to literature data on SCFs in anisotropic carbon fibres is not straightforward. Taking into account the influence of the random fibre packing and distance from the broken fibre, the results coincide well with literature on hexagonal packings [14, 26].

Composites Science and Technology 74 (2013) p. 113-120.
http://dx.doi.org/10.1016/j.compscitech.2012.10.013

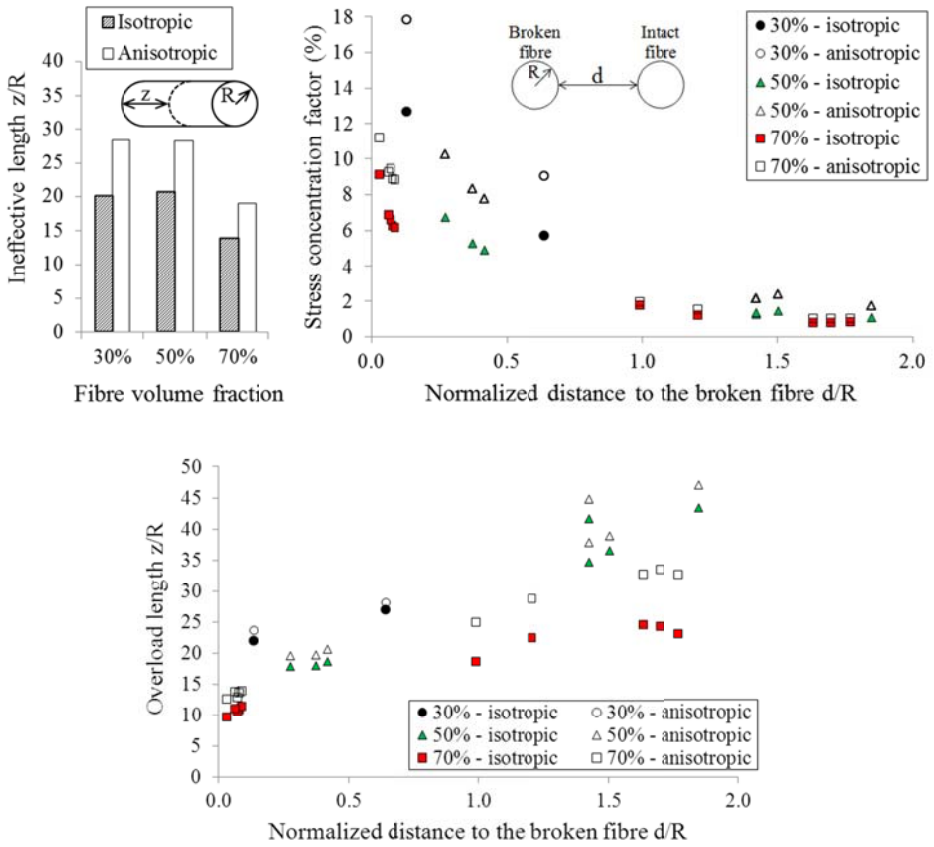

Figure 8: The three parameters describing the stress redistribution for different elastic properties of the fibres: (a) ineffective length (b) SCF (c) overload length.

4 Conclusion

The stress redistribution after a single fibre breakage in various fibre packings was analysed using 3D FEM. Random fibre packings are shown to have significantly different stress concentrations in unidirectional composites with a broken fibre, compared to those for ordered fibre packings. These ordered packings show a higher SCF at the same normalised distance from the broken fibre. Relative differences in SCF of up to 45% were found. However, the highest SCFs were found to be up to 70% higher in random fibre packings. This is because these packings have fibres closer to the broken fibre.

The fibre volume fraction was shown to have an important influence on the SCF, the ineffective and overload length. The influence of the fibre/matrix stiffness ratio is small for the SCF, but important for the ineffective and overload length. Finally, the importance of including anisotropic elastic properties of fibres was illustrated for the case of carbon fibres. Taking into account their anisotropy, they have a significantly higher SCF, ineffective and overload lengths.

Random fibre packings are more realistic representations of unidirectional fibre bundles than ordered packings. They result in significantly different stress redistributions around a broken fibre. The influence of this different stress redistribution on the modelled

strength is however still unclear. The subject of future work is to create a strength model for unidirectional composites with random fibre packings. This model will elucidate whether random fibre packings are needed for an accurate strength model.

5 Acknowledgements

The work leading to this publication has received funding from the European Union Seventh Framework Programme (FP7/2007-2013) under the topic NMP-2009-2.5-1, as part of the project HIVOCOMP (Grant Agreement n° 246389). The authors thank the Agency for Innovation by Science and Technology in Flanders (IWT) for the grant of Y. Swolfs. The authors also thank A.R. Melro and P. Camanho for the permission to use their random fibre packing generator. Thanks are also due to prof. I.M. Ward for the valuable writing advice. I. Verpoest holds the Toray Chair in Composite Materials at KU Leuven.

6 References

[1] Curtin WA. Theory of mechanical properties of ceramic-matrix composites. Journal of the American Ceramic Society. 1991;74(11):2837-2845.
[2] Mishnaevskyjr L, Brondsted P. Micromechanical modeling of damage and fracture of unidirectional fiber reinforced composites: A review. Computational Materials Science. 2009;44(4):1351-1359.
[3] Behzadi S, Curtis PT, Jones FR. Improving the prediction of tensile failure in unidirectional fibre composites by introducing matrix shear yielding. Composites Science and Technology. 2009;69(14):2421-2427.
[4] Hedgepeth JM. Stress concentrations in filamentary structures. NASA TN. 1961;D-882( ):1-36.
[5] Hedgepeth JM, Van Dyke P. Local stress concentrations in imperfect filamentary composite materials. Journal of Composite Materials. 1967;1( ):294-309.
[6] Ryvkin M, Aboudi J. Three-dimensional continuum analysis for a unidirectional composite with a broken fiber. International Journal of Solids and Structures. 2008;45(14-15):4114-4129.
[7] Ohno N. Stress concentrations near a fiber break in unidirectional composites with interfacial slip and matrix yielding. International Journal of Solids and Structures. 2004;41(16-17):4263-4277.
[8] Ochiai S, Hojo M, Osamura K. General expression of the shear lag analysis for unidirectional elastic fiber-elastic matrix composites. Zeitschrift Fur Metallkunde. 1993;84(11):796-801.
[9] Landis CM, McMeeking RM. Stress concentrations in composites with interface sliding, matrix stiffness and uneven fiber spacing using shear lag theory. International Journal of Solids and Structures. 1999;36(28):4333-4361.
[10] Zeng QD, Wang ZL, Ling L. A study of the influence of interfacial damage on stress concentrations in unidirectional composites. Composites Science and Technology. 1997;57(1):129-135.
[11] Okabe T, Takeda N, Kamoshida Y, Shimizu M, Curtin WA. A 3D shear-lag model considering micro-damage and statistical strength prediction of unidirectional fiber-reinforced composites. Composites Science and Technology. 2001;61(12):1773-1787.

[12] Beyerlein IJ, Landis CM. Shear-lag model for failure simulations of unidirectional fiber composites including matrix stiffness. Mechanics of Materials. 1999;31(5):331-350.
[13] de Morais AB. Prediction of the longitudinal tensile strength of polymer matrix composites. Composites Science and Technology. 2006;66(15):2990-2996.
[14] Nedele MR, Wisnom MR. Three-dimensional finite element analysis of the stress concentration at a single fibre break. Composites Science and Technology. 1994;51(4):517-524.
[15] Xia Z, Okabe T, Curtin WA. Shear-lag versus finite element models for stress transfer in fiber-reinforced composites. Composites Science and Technology. 2002;62(9):1141-1149.
[16] van den Heuvel PWJ, Wubbolts MK, Young RJ, Peijs T. Failure phenomena in two-dimensional multi-fibre model composites: 5. A finite element study. Composites Part A-Applied Science and Manufacturing. 1998;29(9-10):1121-1135.
[17] Batdorf SB, Ghaffarian R. Size effect and strength variability of unidirectional composites. International Journal of Fracture. 1984;26(2):113-123.
[18] Fukuda H. Stress concentration factors in unidirectional composites with random fiber spacing. Composites Science and Technology. 1985;22(2):153-163.
[19] Smith RL. The random variation of stress concentration factors in fibrous composites. Journal of Materials Science Letters. 1983;2(8):385-387.
[20] Oh JH, Jin KK, Ha SK. Interfacial strain distribution of a unidirectional composite with randomly distributed fibers under transverse loading. Journal of Composite Materials. 2006;40(9):759-778.
[21] Wongsto A, Li S. Micromechanical FE analysis of UD fibre-reinforced composites with fibres distributed at random over the transverse cross-section. Composites Part a-Applied Science and Manufacturing. 2005;36(9):1246-1266.
[22] Jodrey WS, Tory EM. Computer simulation of close random packing of equal spheres. Physical Review A. 1985;32(4):2347-2351.
[23] Melro AR, Camanho PP, Pinho ST. Generation of random distribution of fibres in long-fibre reinforced composites. Composites Science and Technology. 2008;68(9):2092-2102.
[24] Romanov V, Lomov SL, Gorbatikh L, Verpoest I. Validation of a heuristic fibre placement algorithm: statistical analysis of real and simulated fibre arrangements. XVII International conference on Mechanics of Composite Materials, Book of abstracts, Riga, Latvia 2012.
[25] Xia Z, Curtin WA, Peters PWM. Multiscale modeling of failure in metal matrix composites. Acta Materialia. 2001;49(2):273-287.
[26] van den Heuvel PWJ, Goutianos S, Young RJ, Peijs T. Failure phenomena in fibre-reinforced composites. Part 6: a finite element study of stress concentrations in unidirectional carbon fibre-reinforced epoxy composites. Composites Science and Technology. 2004;64(5):645-656.
[27] Rosen BW. Tensile failure of fibrous composites. Aiaa Journal. 1964;2(11):1985-1991.
[28] Searles K, Odegard G, Kumosa M. Micro- and mesomechanics of 8-harness satin woven fabric composites: I - evaluation of elastic behavior. Composites Part a-Applied Science and Manufacturing. 2001;32(11):1627-1655.

[29] Shindo A. Polyacrylonitrile (PAN)-based carbon fibers. In: Kelly A, Zweben C, Chou TW, editors. Comprehensive composite materials, vol. 1.01 Amsterdam: Elsevier; 2000. p. 1-33.